Accident Analysis and Prevention 200 (2024) 107545

Contents lists available at ScienceDirect

Accident Analysis and Prevention

journal homepage: www.elsevier.com/locate/aap

The role of driver head pose dynamics and instantaneous driving in safety critical events: Application of computer vision in naturalistic driving

Zulqarnain H. Khattak [a,*], Wan Li [b], Thomas Karnowski [b], Asad J. Khattak [c]

[a] Civil and Environmental Engineering, Carnegie Mellon University, United States
[b] Oak Ridge National Laboratory, United States
[c] Civil and Environmental Engineering, University of Tennessee, United States

ARTICLE INFO

Keywords:
Vehicle kinematics
Head pose dynamics
Safety critical
Naturalistic driving
Computer vision
Mixed logit

ABSTRACT

This paper investigates the role of driver behavior especially head pose dynamics in safety–critical events (SCEs). Using a large dataset collected in a naturalistic driving study, this paper analyzes the head pose dynamics and driving behavior in moments leading up to crashes or near-crashes. The study uses advanced computer vision and mixed logit modeling techniques to identify patterns and relationships between drivers' head pose dynamics and crash involvement. The results suggest that driver-head pose dynamics, especially poses that indicate distraction and movement volatility, are important factors that can contribute to undesirable safety outcomes. Marginal effects show that angular deviation for head pose dynamics indicated by yaw, pitch and roll increase the likelihood of crash intensity by 4.56%, 4.92% and 8.26% respectively. Furthermore, traffic flow and lane changing also contribute to increase in likelihood of crash intensity. These findings provide new insights into pre-crash factors, especially human factors and safety–critical events. The study highlights the importance of considering human factors in designing driver assistance systems and developing safer vehicles. This research contributes by examining naturalistic driving data at the microscopic level with early detection of behaviors that lead to SCEs and provides a basis for future research on automation.

1. Introduction

Driver distraction and human error are considered major causes of roadway crashes. While driving is a complex cognitive phenomenon and requires continuous attention of the road, drivers are still observed to be distracted through involvement in various non-driving related tasks such as listening to music, engaging with other passengers, engaging with vehicle consoles, looking at scenic views, cellphone use, and writing etc., among a few (Stutts et al., 2005); (Dingus et al., 2016). Such distractions limit the driver's ability to focus on the task of maneuvering the vehicle and controlling its lateral and longitudinal position (Martin et al., 2013); (Paolo Busardo et al., 2018). Distraction is defined as "the inability of driver to focus on the road due to temporary focus on non-driving related tasks, leading to increased risk of crashes and near-crashes (Regan et al., 2008). These distractions contribute to 23 % of crashes.

The advent of sensing technology and vehicle connectivity and automation offer opportunities to avoid such crashes. Advanced sensors and other in-vehicle devices allow the collection of enormous amounts of data and monitoring of driver state. Such data could be used to monitor driver behavior and identify events that could trigger safety issues. Head pose and gaze behavior is vital in manual driving to assess how the driver is monitoring the environment as well as for partial to full automation to determine situations that require take-over requests and for semantic perceptions. While dynamics of distraction can be represented in different ways, this study represents such driving distraction through driver head pose dynamics involving yaw, pitch and roll. Yaw indicates rotation relative to the vertical axis showing motion of the head in the left and right direction. Likewise, pitch represents angular rotation relative to the lateral axis showing motion in upward and downward direction while roll indicates angular rotation relative to the longitudinal axis showing rotation of head in the left downward and right downward direction. Such head pose dynamics are critical from safety perspective to analyze their correlation with the occurrence of safety–critical events (SCEs). SCEs in this study refers to crashes and near crashes or near misses while SCE intensity refer to severe, major, minor and low risk collision events. When the subject vehicle makes a contact with a moving or fixed object at a certain speed, it is termed a

* Corresponding author.
E-mail addresses: zkhattak@cmu.edu, zk6cq@virginia.edu (Z.H. Khattak).

https://doi.org/10.1016/j.aap.2024.107545
Received 1 May 2023; Received in revised form 17 November 2023; Accepted 10 March 2024
Available online 16 March 2024

crash. Likewise, unwanted behavior that has the potential to cause damage is referred to as near miss. While past studies have developed models for predicting driver head pose dynamics, the role of these head pose dynamics in driving instability and involvement in safety critical events has not been studied. This paper contributes to the literature by estimating head pose dynamics from naturalistic driving using computer vision techniques and analyzing the role of head pose dynamics and volatile driving, represented by abrupt variations in driving regimes, on crash intensity. This research would be helpful in early detection of behaviors leading to SCEs.

2. Literature review

This section is divided into studies utilizing driver head pose and gaze dynamics and their prediction. Further, studies using naturalistic driving data to predict of SCEs are also discussed.

2.1. Studies on head pose and gaze behavior dynamics

The works on gaze dynamics in the literature focus on gaze estimation and gaze behavior modeling. The purpose of eye gaze and head pose dynamics is to identify driver's visual attention. Eye gaze measures the exact location of driver's gaze by tracking eye movement of a driver. The measure is difficult to estimate due to changes in roadway illumination, and occlusion. Head pose provides a measure of visual attention of a driver by estimating head rotation from a central axis. Eye gaze is usually estimated from eye gaze sensors while head pose dynamics utilized in this study have been estimated from recorded in-cabin videos of driver behavior using computer vision techniques. The literature suggest that normal gaze behavior with glances occurring within the center of road may not be safety critical (Birrell and Fowkes, 2014). However, glances to side vehicles during overtaking, or glances to side roads (off-center) and pedestrians within complex urban setting are safety critical. A study (Ahlstrom et al., 2013) classifies gaze into predefined zones using 3D gaze tracking and developed a distraction detection system. They observed that the glance behavior did not change significantly with the distraction detection system. Another study (Vicente et al., 2015) developed a head pose estimation algorithm and conducted gaze evaluations in stationary vehicles using a number of gaze zones for on-road and off-road movement. They observed their algorithm to perform well during a wide variety of conditions. Tawari et al., (2014) used appearance description for state of the eyes to augment head pose and horizontal gaze surrogate for allowing an increased number of gaze zones using naturalistic driving. They observed their tracking method based on video sequence to perform well compared to traditional methods. Another work (Fridman et al., 2016) used a naturalistic dataset to represent eye and head pose dynamics role in gaze classification accuracy. They concluded that adding eye pose along with head pose does not contribute additional classification accuracy when the head moves a lot.

Further, the driver gaze modeling and behavior studies have mostly focused on driving simulators while a few studies have analyzed on-road driving performance. Birrell and Fowkes, (2014) analyzed glance behavior using in-vehicle driving aids. They analyzed glance behavior between baseline, normal, and use of in-vehicle devices through glance transition frequencies. They observed that glances to driving aids did not contribute to additional distraction. Munoz et al., (2016) conducted experimental study to analyze glance allocation under normal driving, radio tuning (manual) and radio tuning (voice based). They observed drivers to maintain high level of attention with voice based technologies compared to manual interface. Li and Busso, (2016) conducted an on-road study and observed different head pose patterns for drivers engaged in secondary tasks as opposed to normal driving. The study also utilized road camera and CAN Bus for analyzing actions corresponding to mirror checking. Another study (Fridman et al., 2017) also analyzed inference of external environment from glance patterns. Martin et al., (2018) analyzed drivers gaze and head pose patterns in freeway driving maneuvers involving left lane changing, lane keeping using naturalistic driving data. The results for modeling these patterns have the ability to detect maneuvers up to a few millimeters. Another study (Rezaei and Klette, 2014) aimed to prevent crashes caused by driver distraction and fatigue by monitoring driver behavior through yawning and head nudging. Their distraction detection algorithm detected behavior based on head pose under different conditions. Zhao et al., (2020) used head pose as a measure of distraction and compared regression with classical neural networks for head pose detection. They observed that head posture for normal driving had statistically significant difference from head posture for distracted driving. Fernández et al., (2016) provided a review of developing monitoring systems to prevent distraction. Recently, Tavakoli and Heydarian, (2022) classified driver reactions based on gaze patterns and under different driving patterns of harsh braking and normal driving. They observed free flow driving to involve lower gaze entropy and normal heart rate.

2.2. Driver behavior and safety related studies from naturalistic driving (NDS)

The relation between traffic, roadway, weather and driving behavior related features and crashes has been analyzed in the literature (Hu and Donnell, 2010); (Gaweesh and Ahmed, 2019); (Hassan et al., 2017; Khattak et al., 2018). Driver behavior has been recognized as a major contributor to crash occurrence (Boyle et al., 2008; Yan et al., 2008). Further, socioeconomic and other driver and age related features have also been identified to contribute to the relation of crashes and distracted behavior (Mitchell et al., 2014; Weng and Meng, 2012). While such assessment is primarily conducted using police reported crashes, such sources may not represent the true factors surrounding these events. The information regarding vehicle kinematics, driver behavior and head pose dynamics is not present in such police reports. Survey questionnaires have also been used in the literature (Scott-Parker and Oviedo-Trespalacios, 2017) to relate crashes and driving behavior (Smorti and Guarnieri, 2014).

The study of safe and unsafe road outcomes has been revolutionized by the development of naturalistic driving data that uses sensors, video technology and radars to generate massive amounts of second-by-second kinematic data (Antin, 2011). This enables identification of behavior before occurrence of SCEs. NDS data has extensively been used to study the impacts of distraction (Fitch et al., 2015; Rakauskas et al., 2004), and behavior under varying speeds (Richard et al., 2020). The crash and near crash detection has also been conducted with kinematics (Khattak et al., 2022; Kluger et al., 2016; Perez et al., 2017) Kluger et al., (2016) used k-means clustering with Fourier Transforms to identify SCEs within time series. They observed 78 % detection of SCEs with this method. Perez et al., (2017) validated multiple thresholds for vehicle kinematic to detect SCEs. They observed their approach to have a low sensitivity and potential to improve SCE detection. Khattak et al., (2022) developed convolutional neural network from kinematics collected from NDS to infer SCEs. They observed ensemble CNN to provide highest accuracy of 95.6 % for crash and near crash detection.

Some studies have focused on volatility related features with NDS. Wali and Khattak, (2020) used NDS to assess how volatility is related to SCEs in school zones. Their results indicated lateral and longitudinal volatility influences safety. Arvin et al. (2019) used 617 NDS events to assess how volatility is related to crash intensity. Their fixed and random parameter models showed that crash risk increases with volatile driving.

While NDS has been used to examine crash risk, the relation between event-based volatility and driving instability is unclear. Likewise, past studies have developed models to predict driver head pose dynamics. However, there is a knowledge gap regarding the relation of distraction extracted from driver head pose dynamics and volatile behavior and their contribution to occurrence of SCEs and the intensity of SCEs. This study therefore, contributes by utilizing driver head pose dynamics extracted using computer vision techniques and links them to vehicle kinematics-based volatility from NDS to explore the relation between driver distraction and instability and their contribution to the occurrence of SCEs and intensity of SCEs.

3. Data description

The data from Naturalistic Driving Study (NDS) was used in this study, which was collected during Strategic Highway Research Program (SHRP 2) and included a total of over 3500 participants from multiple states. A total of 4300 naturalistic driving years were involved over a four years period from 2010 to 2013. Various types of sensors, data acquisition and cameras were used to collect kinematics, and steering data (Antin, 2011).

The data consists of kinematics, roadway features, driving behavior and in-cabin driving video logs. The NDS data collected by Virginia Tech Transportation Institute (VTTI) included 30s of driving events for lateral and longitudinal speeds along with acceleration/deceleration for unsafe outcomes of crashes and near misses while 20s driving events for the baseline cases. Thus, driving behavior in two different categories are resulted; the behavior prior to the unsafe event indicates the true aggressive driving irrespective of the outcome, while the adjustment or driver's reaction to the unsafe event is indicated by the other component. The two sequences of behaviors were differentiated based on impact time or reaction time pre and post involvement in unsafe outcome within the driving profile. The NDS data includes detailed information on driving behavior, roadway environment, traffic conditions, vehicular movement, and environmental factors. These variables were extracted from the videos by well-trained data reductionists however, head pose dynamics for this research were extracted using computer vision techniques by the authors. The data reductionists at Virginia Tech Transportation Institute (VTTI) followed the general estimates procedure from National Highways Traffic Safety Administration (NHTSA) to derive variables on driver behavior, secondary tasks, traffic, and environmental conditions from NDS videos. The data reductionists had basic knowledge on human factors and psychology and were recruited by the VTTI as part-time employees (Hankey et al., 2016). The reductionists were required to pass proficiency test (Hankey et al., 2016) prior to coding. More details are available in (Hankey et al., 2016). There are three main categories of variables in NDS including safety critical events, driver related variables, and roadway environment related variables (Hankey et al., 2016). The fourth category of variables for head pose dynamics were extracted by the authors using computer vision techniques from in-cabin videos. These different sets of data were merged together using a common delimiter of "Event Id" and were used to study the role of such roadway, behavioral and distraction features on driving instability.

- **Safety Critical Event Variables:**

The variables in this category are utilized to establish a relation sequence of events during safety critical events and prior to those events. Variables in this class include nature of event, severity of event, maneuvers prior to the incident, driver's reaction, vehicle control post-maneuver, and fault status of the drivers.

- **Driver Variables:**

The variables class in this category include information about the behavior of subject drivers, their performance, and conditions during a safety critical event and prior to such events. These variables include driving behavior, type and duration of secondary tasks, driver impairment, distraction, aggressiveness, seatbelt use, and steering control.

- **Built and Roadway Environment Variables:**

The NDS also provides information about the roadway environment such as type of locality, density of traffic flow, traffic control devices, lanes of travel, surface conditions, roadway alignment, lighting conditions, and weather.

- **Head pose dynamics:**

The head pose dynamics including yaw, pitch and roll were extracted from the second-by-second driving videos of NDS using computer vision techniques. These head pose dynamics indicate driver distraction by identifying their head poses while maneuvering the vehicle through the roadway. These were extracted from in-vehicle cabin videos of NDS by the authors for the purpose of this research.

A set of randomly selected video events were used to test events. These videos were randomly chosen across different set of events to ensure that there was no bias towards specific time periods or weather conditions. The validity of the data was justified through this verification and descriptive statistics provided in Table 1. Table 1 provides the volatility measures along with head pose dynamics, behavior and other lateral maneuver.

3.1. Performance measures

This study analyzes risky driving behavior using the concept of driving volatility. The volatility measures provide an indication of variations in instantaneous driving regimes. The concept of volatility was used since it serves as a safety surrogate due to indication of erratic vehicular movements and availability prior to SCE occurrence. Thus, higher variations in driving regimes indicates higher volatility, and are indicative of driving instability. Crash count and severity have been found to be positively associated with volatile driving (Khattak et al., 2021). Thus, aggressive driving behavior may be represented by volatile driving and increase collision risk. The available 30s of kinematics were used to estimate volatility measures, which consists of pre-event behavior when any unsafe outcome is not anticipated by the driver while the second portion represents the post-event behavior, where the driver may have lost control and is trying to adjust to the conditions. Figs. 1 and 2 represent an example behavior and most of the events were observed to be triggered within 24–26 s period. The driver reaction was observed at around 22 s as matched with the video files and normalized to 25 s for all events. Several volatility measures have been applied to speed, acceleration (longitudinal and lateral), and jerk (Khattak et al., 2017, 2020a; Khattak and Wali, 2017) such as coefficient of variation, standard deviation quartile variation and time varying stochastic volatility to explore variation in vehicle kinematics. Coefficient of variation is a simple measure of volatility that shows dispersion in the data. The interpretation of coefficient of variation is not useful when dealing with data that is not on ratio scale. Likewise, standard deviation measures simple dispersion and is impacted by outlier causing deviation from measuring the actual dispersion. Time varying stochastic volatility is limited to speed volatility since it cannot be applied to negative values in speed. Quartile variation does not rely on all parts of the data; thus, it fails to capture volatility of the entire time series since it misses 50 % of the data. On the contrary, the volatility measures used in this research are leading indicators of hazards and are different to standard deviation, which makes the construct useful in predicting hazardous situations. Bollinger bands estimates volatile driving relative to moving average over time and provides an efficient way of identifying abrupt variations in driving behavior (Lento et al., 2007). The measures are discussed in detail as follow.

3.1.1. Mean absolute deviation (D_{mean})

The average distance of the observations to the mean is given by:

Table 1
Summary Statistics for Variables.

Variable	Description	Mean	S.D.	Min	Max
Head Pose dynamics					
Yaw	Indicates rotation relative to the vertical axis showing motion of the head in the left and right direction	–23.149	6.146393	−704.42	1171.51
Pitch	Indicates angular rotation relative to the lateral axis showing motion in upward and downward direction.	−0.7940	2.572252	−176.25	150.73
Roll	Indicates angular rotation relative to the longitudinal axis showing rotation of head in the left downward and right downward direction.	0.6511	2.202617	−195.75	236.45
Measures of Volatility (20 sec)					
Positive- Bollinger band-Longitudinal Volatility	Indicates positive portion of Bollinger bands for longitudinal volatility	0.0951	0.0759	0.0146	0.6451
Negative- Bollinger band-Longitudinal Volatility	Indicates negative portion of Bollinger bands for longitudinal volatility	-0.01448	0.02531	−0.2010	0.2088
Positive- Bollinger band-Lateral Volatility	Indicates positive portion of Bollinger bands for lateral volatility	0.0884	0.1036	0.0243	1.019
Negative- Bollinger band-Lateral Volatility	Indicates negative portion of Bollinger bands for lateral volatility	-0.02245	0.03827	−0.5717	0.2574
Longitudinal Vol pos-Mean abs deviation	Indicates positive portion of mean absolute deviation for longitudinal volatility	0.0320	0.0247	0.0144	0.371
Longitudinal Vol neg- Mean abs deviation	Indicates negative portion of mean absolute deviation for longitudinal volatility	−0.0331	0.0212	−0.499	−0.034
Lateral Vol pos- Mean abs deviation	Indicates positive portion of mean absolute deviation for lateral volatility	0.0296	0.0202	0.0143	0.3518
Lateral Vol neg – Mean abs deviation	Indicates negative portion of mean absolute deviation for lateral volatility	-0.03202	0.02174	−0.4509	−0.0746
Measures of Volatility (30 sec)					
Positive- Bollinger band-Longitudinal Volatility	Indicates positive portion of Bollinger bands for longitudinal volatility	0.106	0.085	0.000	1.948
Negative- Bollinger band-Longitudinal Volatility	Indicates negative portion of Bollinger bands for longitudinal volatility	−0.019	0.032	−1.338	0.210
Positive- Bollinger band-Lateral Volatility	Indicates positive portion of Bollinger bands for lateral volatility	0.100	0.114	0.000	1.106
Negative- Bollinger band-Lateral Volatility	Indicates negative portion of Bollinger bands for lateral volatility	−0.029	0.049	−0.665	0.257
Positive-jerk- Longitudinal Volatility	Indicates positive portion of Jerk for longitudinal volatility	0.039	0.032	0.000	0.338
Negative-jerk- Longitudinal Volatility	Indicates negative portion of Jerk for longitudinal volatility	−0.040	0.029	−0.456	0.000
Positive-jerk- Lateral Volatility	Indicates positive portion of Jerk for lateral volatility	0.032	0.023	0.000	0.495
Negative -jerk- Lateral Volatility	Indicates negative portion of Jerk for lateral volatility	−0.035	0.025	−0.451	−0.843
Driver Behavior					
Aggressive	Represents driver aggressive behavior while maneuvering the vehicle	0.005	0.072	0.000	1.000
Distraction	Represents distracted drivers during vehicle maneuvering due to activities deemed unnecessary. Derived from video repositories	0.071	0.257	0.000	1.000
Anger	Represents angry driver behavior caused by personal or roadway characteristics. This indicator was derived from video repositories based on driver’s expression and their response to roadway conditions.	0.005	0.071	0.000	1.000
Inexperienced and unfamiliar	Represents inexperienced drivers. This was derived from video repositories based on experience and driving skills.	0.006	0.076	0.000	1.000
Safe maneuver	Represents an unharmful maneuver for the driver or other roadway users. This was derived from video repositories by ranking unsafe and safe maneuvers	0.893	0.309	0.000	1.000
Illegal maneuver	Represents a harmful maneuver for roadway participants that may be deemed illegal. This was derived from video repositories	0.021	0.142	0.000	1.000
Lateral Maneuvers					
Lane change	Represents a lane changing maneuver. This was derived from video repositories	0.038	0.191	0.000	1.000
Merge	Represents a merge maneuver onto the mainline traffic from a ramp or merge action between vehicles within mainline traffic. This was derived from video repositories	0.032	0.059	0.000	1.000
Overtaking	Represents an overtaking maneuver. This was derived from video repositories	0.005	0.071	0.000	1.000
Curve negotiation	Representing a curve negotiation action performed by the driver. This was derived from video repositories	0.087	0.282	0.000	1.000
Secondary Task					
Secondary task 1 duration	Represents time spent on non-essential tasks while driving that are termed as secondary tasks. This indicates the first among the two classified tasks	2.092	2.720	−2.470	24.119
Secondary task 2 duration	Represents the amount of time spent on the second category of a secondary task	0.354	1.251	0.000	14.221
Texting	Represents texting activity while driving.	0.023	0.149	0.000	1.000

(*continued on next page*)

Table 1 (*continued*)

Variable	Description	Mean	S.D.	Min	Max
Cellphone use	Represents cell phone use activity	0.071	0.257	0.000	1.000
Density (Traffic)					
LOS A- Free flow	Represents traffic that is free flow, indicated by level of service A	0.706	0.456	0.000	1.000
LOS B- Stable	Represents traffic that is stable flow, indicated by level of service B	0.261	0.439	0.000	1.000
LOS F - Unstable	Represents traffic that is unstable or close to conditions of breakdown, indicated by level of service F	0.031	0.172	0.000	1.000
Roadway Features					
Divided roadway	Representing a divided roadway	0.400	0.490	0.000	1.000
Traffic signals	Represents the presence of traffic signals	0.105	0.306	0.000	1.000
Construction	Represents the presence of construction activity	0.021	0.143	0.000	1.000
Stop sign	Represents the presence of stop signs	0.032	0.177	0.000	1.000
Driveway	Represents the presence of driveways	0.065	0.247	0.000	1.000
Interchange	Represents the presence of interchange	0.066	0.248	0.000	1.000
Weather and Lighting					
Weather (adverse)	Represents the presence of adverse weather conditions	0.103	0.304	0.000	1.000
Dark	Represents the presence of dark conditions	0.240	0.427	0.000	1.000

$$D_{mean} = \frac{1}{n}\sum\nolimits_{i=1}^{n} |x_i - \overline{x}| \quad (1)$$

This measure is applied to vehicular speed, deceleration, and acceleration.

3.1.2. Bollinger bands

Bollinger bands (Lento et al., 2007) are used to relate speeds and acceleration to driving volatility(relative average). The volatility level is represented by the standard deviation and width of the band (Fig. 3) while higher or lower standard deviation across the mean represents the volatility. Thus, resulting in upper bound (BB_u) and lower band (BB_l) around the mean provided in equation (2) and (3).

$$BB_u = MA + 2\sqrt{\frac{\left(\frac{(x_i - MA)^2}{n}\right)^2}{n}} \quad (2)$$

$$BB_l = MA - 2\sqrt{\frac{(x_i - MA)^2}{n}} \quad (3)$$

where acceleration or speed at any instant are given by x, and n indicates the total observations. The moving average (MA) is given by equation (4), which was estimated using timeseries with several 5 s chunks. For instance, the initial 5 s (1 s-5 s) of the series were used to estimate MA, later the next 5 s (i.e., 2 s-6 s) chunk of the = series was used to estimate MA. Furthermore, MA was estimated using multiple chunks of series. The time series accounts for the change in volatility while the Bollinger Bands (upper and lower) were estimated using the moving average.

$$MA = \sum_{i=1}^{n} \left(\frac{\sum_{i}^{i+4} x_i}{5} \right) \Big/ n \quad (4)$$

The volatility measures used in this research are kinematics-based indicators of hazards and are different to standard deviation, which makes the construct useful in predicting hazardous situations. However, the measures have some limitations. Bollinger bands has a reactive nature as these measures react to sudden changes in speed profiles (i.e., downwards or upward trends) since they take moving average of speed profiles. Likewise, the limitation of using mean absolute deviation is their dependence on median, which makes the results unsatisfactory when the deviations are very high.

4. Methodological description

This section discusses the extraction of head pose dynamics and modeling approach for relation of head pose dynamics with safety critical events and crash intensity.

4.1. Computer vision for extraction of head pose dynamics

The face characterization data was extracted using the Retina face algorithm (Deng et al., 2020) implemented within the “Face Recognition Oak Ridge” (FaRO) framework (Bolme et al., 2020) on the second by second driving from NDS. This method extracted the face location as well as facial key points. The head pose dynamics (angular yaw, pitch, and roll) were extracted using the “Hopenet” method (Ruiz et al., 2018), also implemented in the FaRO framework. The general process can be defined as, given a set of in-cabin face images $j = \{j_n | n = 1, \cdots, N\}$ and the pose vector y_n comprising the yaw, pitch and roll angles, denoted as $\varphi, \theta and \gamma$. The goal is to minimize the mean absolute error (MAE) through a mapping function F with respect to ground truth y and estimation $y' = F(x)$.

$$F(X) = \frac{1}{N}\sum\nolimits_{i=1}^{N} \| \varphi' - \varphi | + |\theta' - \theta| + |\gamma' - \gamma| \quad (5)$$

where φ', θ' and γ' indicate the estimates of y_i' after the evaluation target is split into three angles.

Fig. 4 shows the architecture of detailed approach (Ruiz et al., 2018). The method relies on estimation of angular position of the passenger’s head in-cabin to initiate noise control. The first step involves facial landmark approach where the face detection is performed, and critical landmarks or key points are identified. The second step involves estimation of head angular rotations, face identification and Euler angles. The fixed size image passes through the model to generate a feature map at each stage of the backbone network. The features extracted from the neighboring states are fused using down sampling and max pooling. The three Euler angles are differentiated based on external feature selection. The head pose estimation from regression angles mean squared error loss, which is commonly used is not satisfactory for large scale data. Each loss consists of a classification and regression component. A backbone network is then used to augment with the fully connected layer. The previous convolutional layers (Emu et al., 2022; Haydari et al., 2021) of the network are shared by these fully connected layers (Ruiz et al., 2018). The pose within the neighborhood is predicted in an efficient manner by having soft-max and cross entropy layers that performs bin classification. The learning process is improved by

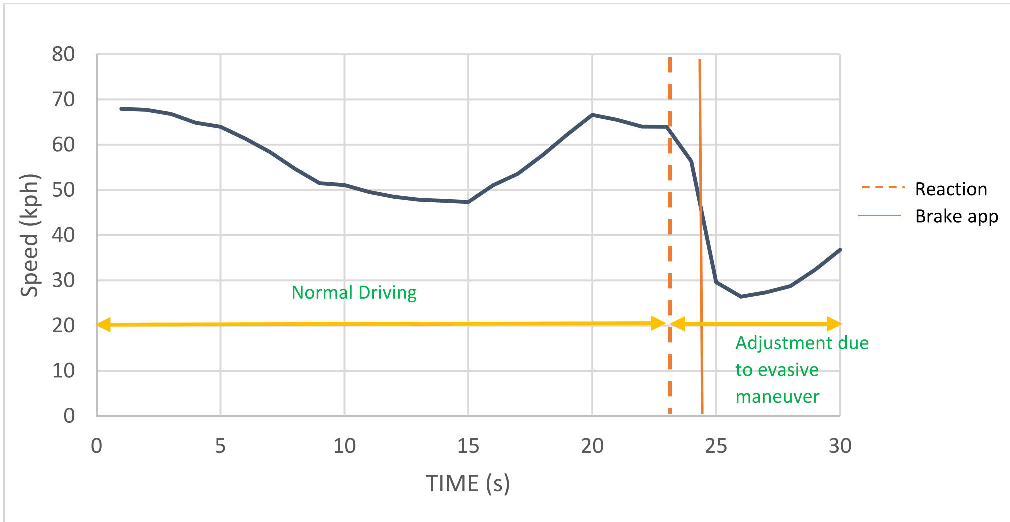

a) Speed Profile for near crash

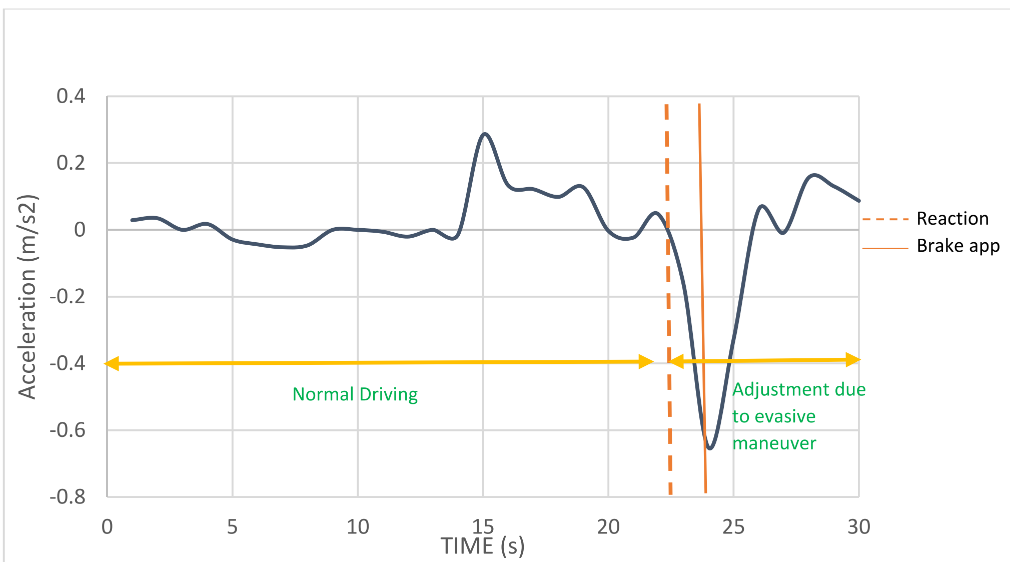

b) Acceleration Profile for near crash

Fig. 1. Kinematics for a near Crash event.

back-propagating three angles through separate cross entropy losses. The binned output is used to calculate the expected output angle. The predictions are further improved by adding a mean squared error loss to the network. Each angle (yaw, pitch and roll) has a separate loss, which is composed of regression and classification loss. The final Euler loss angle is given by equation (6) (Ruiz et al., 2018).

$$\mathscr{L} = H(y, \hat{y}) + \alpha.MSE(y, \hat{y}) \tag{6}$$

4.2. Modeling role of head pose dynamics on safety critical events

The study motivation is to assess the association between distraction resulting from head pose dynamics and driving instability and their contribution towards SCE intensity. The overall framework is shown in Fig. 5. The head pose dynamics and volatility can be utilized to detect any anomalous behavior and provide alerts to reduce driving instability and the occurrence of SCEs. This monitoring phenomenon can be used to analyze instantaneous driving, and provide alerts based on hotspots identified with highly volatile driving. This would enable to establish countermeasures for reducing such behavior. From a modeling perspective, the relation between head pose dynamics and driving instability was modeled using Tobit model due to volatility measures being left censored at zero. The model is widely used in the literature for censored data and was proposed by (Tobin, 1958). We can write equation (6) based on left-censored limit.

$$Y_{1,i} = \alpha_1 + \beta_1 X_1 + \varepsilon_i, \mathrm{i} = 1, 2, 3, \cdots\cdots, \mathrm{N} \tag{7}$$

$$Y_{1,i} = Y^*_{1,i} if Y^*_{1,i} > 0 \tag{8}$$

$$Y_{1,i} = Y^*_{1,i} if Y^*_{1,i} \leq 0 \tag{9}$$

where α_1 indicates intercept, the volatility is indicated by Y_1 and the head pose dynamics and other roadway, and environment related factors are indicated by X_1. N indicates the observations while ε_i indicates the normally distributed error. The likelihood function is given by equation (9) with σ indicating normal density function:

$$Likelihood = \prod_0 \left[1 - \varnothing\left(\frac{\beta X}{\sigma}\right)\right] \prod_0 \left[\sigma^{-1} \varnothing\left(\frac{Y_i - \beta X}{\sigma}\right)\right] \tag{10}$$

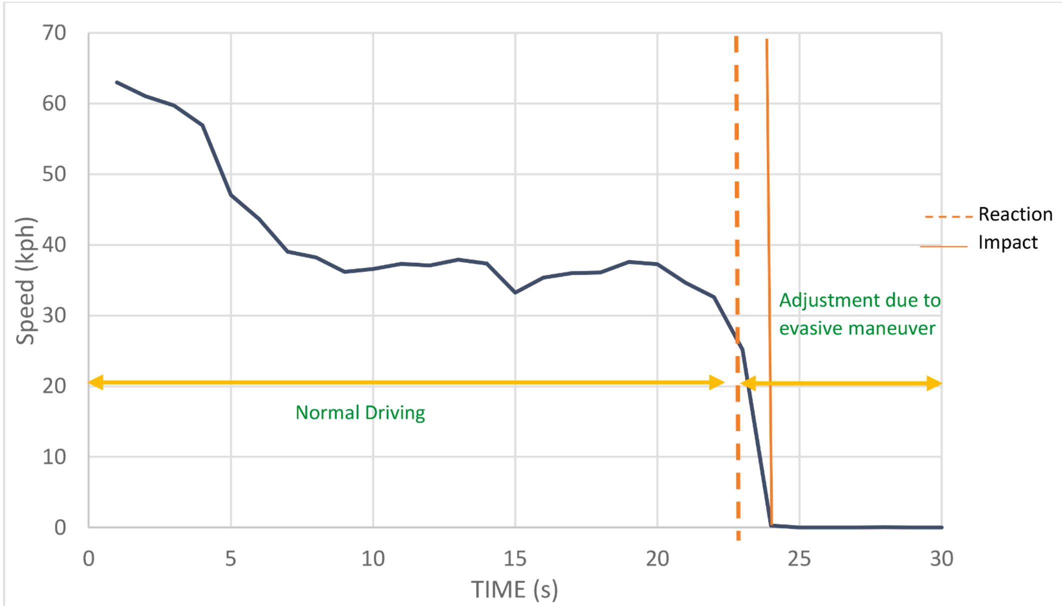

a) Speed Profile for crash

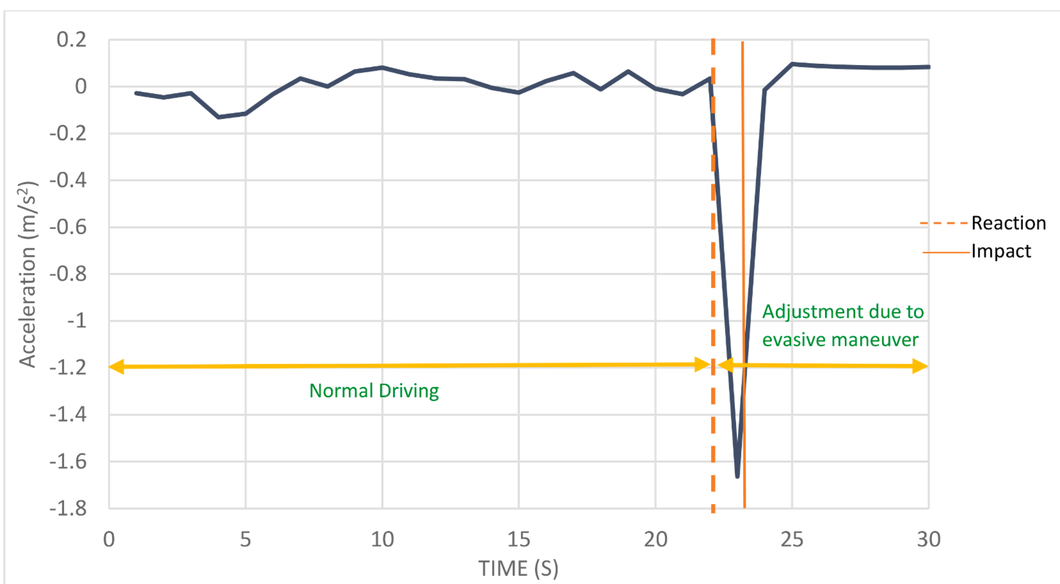

b) Acceleration Profile for crash

Fig. 2. Kinematics for a crash event.

where β represents the coefficient and X represents the variable of interest including head pose dynamics, driving behavior factors, weather and roadway features etc.

Further, the association of head pose dynamics and volatility with crash intensity was conducted using a mixed logit model. This is widely used method based on the categorical nature of the dependent variable of crash intensity (Ben-Akiva and Lerman, 1985; Washington et al., 2011). The dependent variable of crash intensity includes severe, police reportable, minor, and low risk along with baseline. The mixed logit approach takes unobserved heterogeneity (Khattak et al., 2021) into account by allowing the estimated parameters to vary (Ukkusuri et al., 2011) given by equation (11).

$$Y_{in} = \beta_i X_{in} + \varepsilon_{ij} + n_{in} \tag{11}$$

where the random term with specific distribution is given by n_{in}, the crash intensity function is crash n with the event categories i given by Y_{ij}, the explanatory variables are given by X_{in} (Ben-Akiva and Lerman, 1985), the coefficient is given by β_i while ε_{ij} gives the unobserved effects.

The probability is given by equation (12) based on the random term distribution assumption (Train, 2003).

$$P_j(i) = \frac{\exp(\beta_i X_{ij})}{\sum_I \exp(\beta_i X_{ij})} f(\beta|\varnothing) d\beta \tag{12}$$

where $f(\beta|\varnothing)$ represents the joint density function while β and $\varnothing$ indicates the density function's vector parameter (Washington et al., 2011). The unobserved heterogeneity is accounted for using the density function (Train, 2003). Among the different functional forms, the normal distribution $\beta_{ij\ Normal(\beta_{j,\sigma^2})}$ was selected for random parameters

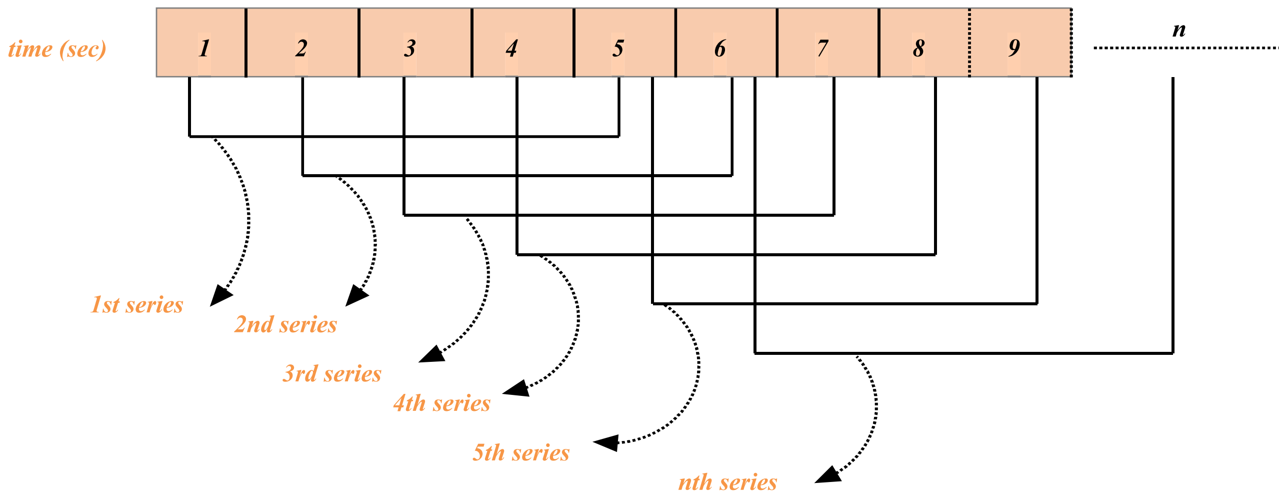

Fig. 3. Bollinger Bands estimation through moving average.

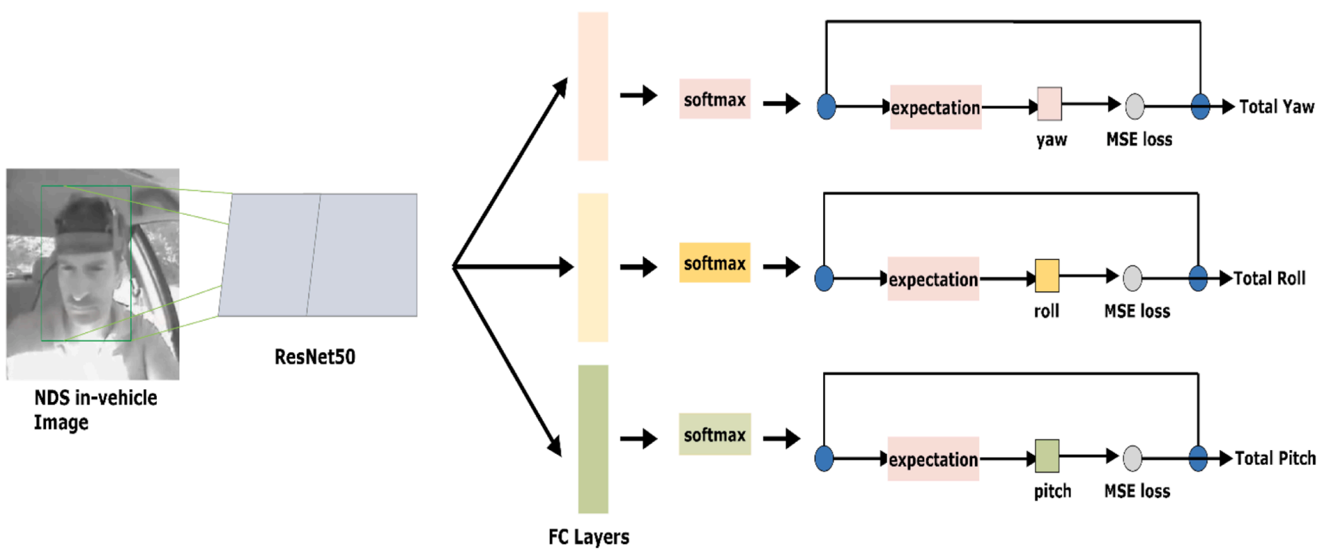

Fig. 4. Head Pose dynamics extraction using Hopenet method (Ruiz et al., 2018).

due to better fit (Ahmed et al., 2018; Xie et al., 2018). The random parameters were estimated using 200 Halton draws from simulation based maximum likelihood (Halton, 1960; Train, 2003). Marginal effects were further used to interpret the propensity change of intermediate categories. A 0-1unit difference is used to interpret the dummy variable change while a continuous variable is indicated by change of one standard deviation from the mean. A value below 0.80 for correlation and low multicollinearity (Washington et al., 2011) shown by a variance of inflation below 2 were used (Chatterjee and Hadi, 2015; Greene, 2008; Khattak et al., 2017) as criterions for variable selection.

5. Results and discussion

The results for head pose dynamics and the modeling estimates are discussed in this section.

5.1. Description of Retina face dynamics

This section shows a few examples of extracted head pose dynamics and their accuracy statistics. For privacy concerns, the images have been anonymized. Fig. 6 represents the accuracy of head pose dynamics extracted from second-by-second naturalistic driving. The estimates for the mean average error of the Euler angles based on Multi-Loss ResNet50 were in the range of 5.4 to 6.5 degrees while the mean absolute error was 6.1 degrees. All these errors are in lower range indicating higher accuracy of the estimated head pose dynamics. The accuracy of the extracted head pose dynamics in Fig. 6 was observed to be similar to (Ruiz et al., 2018). Fig. 7 shows examples of extracted head pose dynamics that are illustrated through computer graphic heads in a variety of examples of different head pose angles (*https://facegen.com/*). Fig. 7a indicates a driver looking straight ahead towards the road with a yaw angle of zero and pitch angle of 10, Fig. 7b indicates a driver looking at the dashboard console with a yaw angle of zero and pitch angle of 40 while Fig. 7c indicates a driver looking towards right with a yaw angle of 40 and pitch of zero. These examples represent only a few cases out of several scenarios for the extracted head pose dynamics that indicate drivers' level of distraction.

5.2. Modeling results

This section provides the results for role of distraction extracted from head pose dynamics on driving instability and involvement in SCEs.

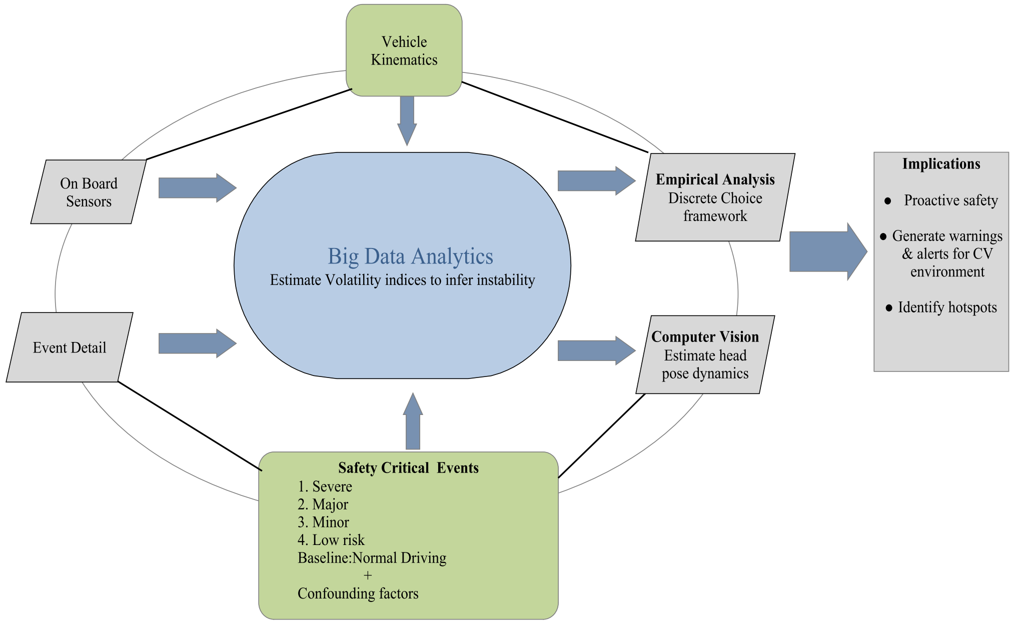

Fig. 5. Framework for Analysis.

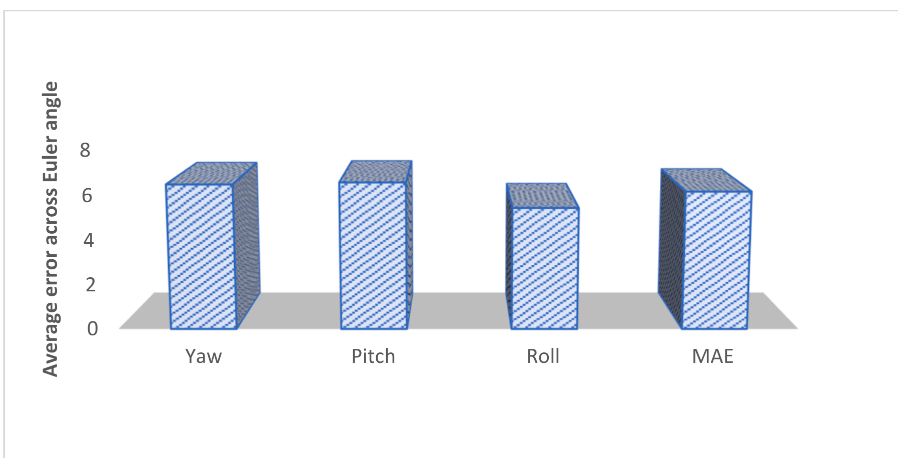

Fig. 6. Average Euler error (degrees) with Multi-Loss ResNet50.

Volatility measures are leading indicators of safety due to their availability prior to SCEs occurrence and representation of three dimensional erratic vehicular movements. Their ability to predict short-term driving decisions prior to occurrence of unsafe outcomes helps in mapping volatility to drivers' involvement in unsafe outcomes for understanding the maneuvers and behaviors leading to SCE. Thus, the influence of higher or lower volatility on the probability of intense crash was investigated. Furthermore, multiple volatility measures were calculated using vehicle kinematics from NDS to assess the volatility and SCE relation.

5.2.1. Driving instability

The discussion of the role of distraction extracted from head pose dynamics on driving instability is provided in this section. The driving instability, measured as speed volatility serves as the dependent variable. Volatile driving represents abrupt variation in driving regimes that could result in SCEs. The modeling results are provided in Table 2 for the Tobit model. The results reveal that head pose dynamics are highly associated with driving instability. All three measures of head pose dynamics (yaw, pitch, and roll) show relation to increase in driving instability represented by driving volatility, which may contribute to SCEs. A unit increase in yaw representing rotation relative to the vertical axis shows a 1.06 unit increase in driving instability. This is intuitive since the driver is highly distracted with increase in yaw dynamics while looking left or right at the external roadway environment as opposed to keeping a straight head position. Likewise, a unit increase in pitch indicating angular rotation relative to the lateral axis shows 0.35 units increase in driving instability represented by volatile driving This is also intuitive since driver is distracted from the road while moving their head up and down looking at the vehicle console or other components inside the vehicles. Further, a unit increase in roll indicating angular rotation relative to the longitudinal axis shows 0.54 units increase in driving instability. This is also intuitive since rotating head left or right downwards while looking at the passengers or at the back seats also results in distraction. The distractions indicated by these head pose dynamics increase workload and reduces driver's attention to concentrate on the driving tasks, which could result in driving instability and ultimately contribute to occurrence of SCEs.

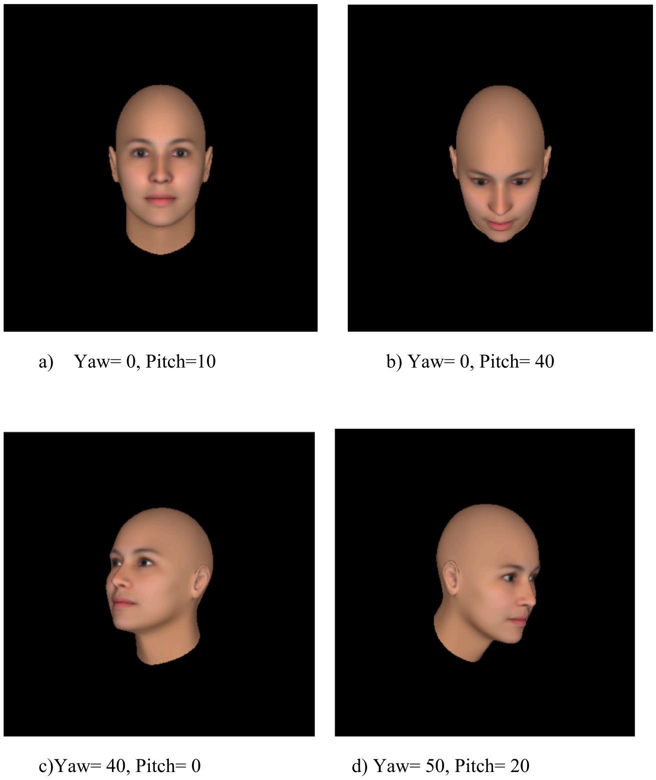

Fig. 7. Example head pose dynamics.

Table 2
Tobit Model for studying the role of head pose dynamics on driving instability.

Variable	Tobit Model	
	Coeff	p-value
Head Pose dynamics		
Yaw	1.06	<0.01
Pitch	0.35	<0.01
Roll	0.54	0.07
Behavioral Parameters		
Variable for Lane change	1.02	<0.05
Variable for Inexperience	0.63	0.07
Traffic Density		
Variable representing Free flow (LOS A)	−2.45	<0.01
Variable representing Unstable flow (LOS F)	1.28	<0.01
Roadway Features		
Variable for Divided roadway	−0.91	0.06
Variable for Traffic signals	0.71	0.07
Weather and Lighting		
Variable for Adverse weather	0.20	0.06
Summary Statistics		
Log likelihood at Null	−7456.21	
Log likelihood at Convergence	−5321.4	
AIC	2032	

Furthermore, other control variables also show association with driving instability. For instance, lane changing is observed to increase driving instability by 1.02 units. Lane changing is a complex phenomenon, and some degree of instability is expected during lane change maneuvers. Likewise, traffic flow is also observed to contribute significantly towards driving instability. While driving is expected to be stable during free flow conditions, the level of service F indicating breakdown increases driving instability by 1.28 units. Further, urban settings with traffic signals also increase the likelihood of driving instability as opposed to freeway driving. A unit increase in driving within dense urban areas with traffic signals increases driving instability by 0.71 units. This may be attributed to continuous stop and go waves created by poor signal coordination or multiple conflicting movements during peak hours.

5.2.2. Role of head pose dynamics on involvement in safety critical events

While the previous section assesses the relation of driver's head pose dynamics and driving instability, it is important to analyze driver distraction's role extracted from head pose dynamics, volatility, and other associated factors on SCE intensity. Using a large dataset collected in a naturalistic driving study, this paper analyzes the head pose dynamics and driving behavior in moments leading up to crashes or near-crashes. The kinematics data included three classes of events namely crashes, near misses and baselines. Furthermore, video frames were also available for each of the three classes of data. The head pose dynamics for each of the events within the time frame of 30 s prior to occurrence of the crash and near miss event were extracted from the in-cabin videos for all of the available events and the event selection was not biased based on contribution of head pose dynamics towards unsafe outcomes. Thus, the analysis provided an indication of whether head pose dynamics had any contribution or influence on the occurrence of crashes or near misses. Table 3 provides the fixed and random parameter models. The AIC values reveal the superiority of random parameter model compared to the fixed parameter model. While lower AIC values are representative of better model fit during comparison of two models using the same dataset, the absolute value of AIC (higher or lower) is meaningless since it is only useful during comparison of two models.

The driving distraction as indicated by head pose dynamics is observed to be associated with increasing the risk of crash intensity. Higher variation in driver distraction as indicated by head pose dynamics of yaw, pitch and roll increases the risk of involvement in severe crashes. Marginal effects reveal that yaw, pitch and roll increase severe crashes by 4.56 %, 4.92 % and 8.26 % respectively. These head pose dynamics indicates angular deviation of driver's head pose from straight view of road towards the left or right of roadway environment, vehicle console elements or involvement with other passengers, which could result in distraction and increases the risk of involvement in severe crashes. Likewise, highly volatile driving is also associated with increased risk of severe crashes. Higher variations in driving regimes indicated by volatility leads to inability of driver to control the vehicle during critical edge cases, which increases the likelihood of severe crashes. Behavioral parameters such as lane changing, and inexperienced driving also contribute to crash severity. Marginal effects reveal that likelihood of minor and low risk crashes increase by 6.95 % and 5.45 % with a unit increase in lane change events while the severe crash likelihood increase by 1.25 % with a unit increase in inexperienced driving as opposed to minor crashes. This is intuitive since inexperienced drivers are not able to maneuver the vehicle properly under critical and complex driving conditions while lane changing by itself is a complex phenomenon and requires attentive and skilled drivers. Adverse weather conditions are also observed to contribute significantly to severe crashes. Marginal effects indicate a 0.86 % increase in severe crashes with a unit increase in adverse weather including rain and snow. Likewise, driving on urban streets with traffic signals also increases the likelihood of severe crashes by 6.41 % as opposed to minor and baseline events. This may be attributed to excessive stop and go traffic resulting from multiple traffic signals on urban streets. Traffic flow is another important contributory factor to severe crashes. Breakdown traffic at LOS F resulting from congestion increases the likelihood of severe crashes by 3.1% as compared to minor and baseline categories. This is intuitive since poor traffic conditions create complex driving conditions that could result in excessive incidents and increase severe crash propensity.

6. Conclusions and limitations

In-vehicle sensor data has created numerous opportunities for studying the relationship between driver behavior and distraction and

Table 3
Modeling results for volatility indices with 20 s data. SE = Severe, MP = Major Police reportable, MI = Minor, LR = Low risk.

Variable	Fixed Parameters Logit		Mixed Logit		Marginal Effects for Mixed Logit				
	Coeff	p-value	Coeff	p-value	Severe	Major	Minor	Low risk	Baseline
Head pose dynamics									
Yaw	0.04	<0.05	0.03	<0.05	0.0456	0.0381	0.0134	−0.0116	−0.0855
Pitch	−0.02	0.195	0.02	<0.05	0.0492	0.0431	0.0116	−0.0150	−0.0889
Roll	0.09	0.084	0.05	0.056	0.0826	0.0106	0.0755	0.0029	−0.1716
Volatility measures									
Lateral volatility pos- Mean Abs deviation [SE]	1.03	0.066	1.02	<0.01	0.4700	0.5420	0.7586	0.4017	−2.1723
Pos Bollinger Band [MP]	−2.54	<0.05	0.54	0.06	0.1782	0.1853	0.1906	0.0931	−0.6472
Neg Bollinger Band [MP]	1.14	0.11	0.45	0.08	−0.3569	−0.3588	−0.1658	−0.2779	1.1594
Driver Behavior									
Lane change [MP]	0.21	0.047	1.01	<0.05	−0.0856	0.0695	0.0545	0.0408	−0.0792
Driving (inexperienced)[MP]	1.42	<0.05	0.54	0.06	0.0124	0.0217	0.0740	0.0435	−0.1516
Traffic Density									
LOS A- Free flow [SE]	−0.79	<0.05	−1.13	<0.05	−0.0094	−0.0166	0.0187	0.0146	−0.0073
LOS F- Unstable [MI]	–	–	−0.48	<0.01	0.0310	0.0401	0.5039	−0.2959	−0.2791
Roadway Features									
Urban/residential [LR]	−0.13	0.13	0.60	0.07	0.0641	0.0224	0.0770	−0.0202	−0.1433
Weather									
Adverse weather [MP]	–	–	0.15	<0.05	0.0084	0.0171	0.0055	0.0116	−0.0426
Unobserved effects (Standard deviation)									
Vol-Mean absolute deviation	–	–	0.66	<0.05	–	–	–		
Vol pos- Bollinger band			0.21	0.053					
Inexperienced	–	–	0.46	<0.05	–	–	–		
Statistics									
Log likelihood (null)	−27806.71		−27806.71		NA	NA	NA	NA	NA
Log likelihood (convergence)	−22732.47		−19831.52		NA	NA	NA	NA	NA
AIC	47,247		39,691		NA	NA	NA	NA	NA

instability prior to SCE occurrence. This study harnessed big data from multiple sources; including, event data, kinematics from second-by-second trajectories and computer vision-based extraction of head pose dynamics. The non-availability of pre-crash information in traditional police reported crashes makes this data unique. The analytic framework is generated using detailed microscopic data to assess the role of distractions extracted from head pose dynamics in driving instability and safety. This study specifically assesses the role of head pose dynamics extracted using computer vision techniques in contributing towards driving instability and safety critical events. While past studies have developed models for predicting driver head pose dynamics, the role of these head pose dynamics on driving instability and involvement in safety critical events has not been studied. This paper contributes by predicting head pose dynamics from naturalistic driving using computer vision techniques and analyzing role of head pose dynamics and volatile driving represented by abrupt variations in driving regimes on the occurrence of SCEs and their intensity. The naturalistic driving data was analyzed for the contribution of pre-crash head pose dynamics towards driving instability and safety. The modeling results reveal a strong association between head pose dynamics and driving instability resulting in severe crashes. Specifically, the likelihood of driving instability is increased significantly by higher variation in head pose dynamics, deviating from baseline values with drivers looking straight towards the front view of the road. This distracted behavior indicated by head pose dynamics is also observed to increase the risk of severe crashes. Furthermore, volatile driving is also observed to increase the propensity of severe crashes. Likewise, involvement in lane changing events and unstable traffic flow on the road are also observed to contribute towards increasing the propensity of severe crashes.

These findings may help in improving proactive safety and impact emerging technologies and practitioners. Technology developers can device mechanisms to monitor head pose dynamics and behavior to detect any anomalous behavior and provide alerts to reduce driving instability and the occurrence of SCEs. This monitoring phenomenon can be used to analyze instantaneous driving, and provide alerts based on highly volatile driving. The monitoring phenomenon can potentially be used to detect pre-crash behaviors resulting in SCEs and improve the connected vehicles performance (Khattak et al., 2020b) since connected vehicles are expected to provide potential warnings and alerts based on surrounding traffic conditions. However, this is still an open topic for research. Practitioners can utilize the results to reduce the distraction arising due to roadway geometry features. The volatility concept can be cross-fertilized across other safety fields, e.g., commercial driver's safety and safety of construction workers, to study mechanisms resulting incidents or crashes. It should be noted that both machine learning and simulation based discrete choice methods can be used for prediction. However, machine learning methods do not indicate the influence of each explanatory factor on dependent variable (driving instability and SCE intensity in our case). The inferential nature of discrete choice or econometric methods serves well in this regard to capture the complex dependencies in the data while attributing the influence of each confounding factor.

CRediT authorship contribution statement

Zulqarnain H. Khattak: Conceptualization, Formal analysis, Funding acquisition, Investigation, Methodology, Project administration, Supervision, Writing – original draft, Writing – review & editing. **Wan Li:** Formal analysis. **Thomas Karnowski:** Formal analysis, Writing – review & editing. **Asad J. Khattak:** Writing – review & editing.

Declaration of competing interest

The authors declare that they have no known competing financial interests or personal relationships that could have appeared to influence the work reported in this paper.

Data availability

Data will be made available on request.

Acknowledgement

The research was funded through the Federal Highway Administration. The research also received support from Collaborative Sciences Center for Road Safety. The project is funded in part by Carnegie Mellon

University's Safety21 National University Transportation Center, which is sponsored by the US Department of Transportation. The authors are thankful for the funding support.

References

Ahlstrom, C., Kircher, K., Kircher, A., 2013. A gaze-based driver distraction warning system and its effect on visual behavior. IEEE Trans. Intell. Transp. Syst. 14.

Ahmed, M.M., Franke, R., Ksaibati, K., Shinstine, D.S., 2018. Effects of truck traffic on crash injury severity on rural highways in Wyoming using Bayesian binary logit models. Accid. Anal. Prev. 117, 106–113. https://doi.org/10.1016/j.aap.2018.04.011.

Antin, J.F., 2011. Design of the in-vehicle driving behavior and crash risk study. Strategic Highway Research Program.

Arvin, R., Kamrani, M., Khattak, A.J., 2019. The role of pre-crash driving instability in contributing to crash intensity using naturalistic driving data. Accident Analysis and Prevention 132 April , 105226. doi:10.1016/j.aap.2019.07.002.

Ben-Akiva, M., Lerman, S.R., 1985. Discrete choice analysis. MIT Press.

Birrell, S.A., Fowkes, M., 2014. Glance behaviours when using an in-vehicle smart driving aid: a real-world, on-road driving study. Transp. Res. Part F: Traffic Psychology and Behavior 22.

Bolme, D.S., Srinivas, N., Brogan, J., Cornett, D., 2020. Face recognition oak ridge (FaRO): a framework for distributed and scalable biometrics applications, in: IEEE International Joint Conference on Biometrics (IJCB). doi:10.1109/IJCB48548.2020.9304933.

Boyle, L.N., Tippin, J., Paul, A., Rizzo, M., 2008. Driver performance in the moments surrounding a microsleep. Transp. Res. F 11.

Chatterjee, S., Hadi, A.S., 2015. Regression analysis by example, 5th Editio. ed.

Deng, J., Guo, J., Ververas, E., Kotsia, I., Zafeiriou, S., 2020. RetinaFace: single-shot multi-level face localisation in the Wild, in: IEEE/CVF Conference on Computer Vision and Pattern Recognition.

Dingus, T.A., Guo, F., Lee, S., Antin, J.F., Perez, M., Buchanan-King, M., Hankey, J., 2016. Driver crash risk factors and prevalence evaluation using naturalistic driving environment. Procedings of National Academy of Sciences 113.

Emu, M., Kamal, F., Choudhury, S., Rahman, Q., 2022. Fatality Prediction for Motor Vehicle Collisions: Mining Big Data Using Deep Learning and Ensemble Methods. IEEE Open J. Intelligent Transp. Syst. 3 https://doi.org/10.1109/OJITS.2022.3160404.

Fernández, A., Usamentiaga, R., Carús, J.L., Casado, R., 2016. Driver distraction using visual-based sensors and algorithms. Sensors 1805. https://doi.org/10.3390/s16111805.

Fitch, G.M., Bartholomew, P.R., Hanowski, R.J., Perez, M.A., 2015. Drivers' visual behavior when using handheld and hands-free cell phones. J. Saf. Res. 105.

Fridman, L., Toyoda, H., Seaman, S., Seppelt, B., Angell, L., Lee, J., Mehler, B., Reimer, B., 2017. What can be predicted from six seconds of driver glances?, in: CHI Conf. Human Factors Comput. Systems.

Fridman, L., Lee, J., Reimer, B., Victor, T., 2016. Owl and lizard: patterns of head pose and eye pose in driver gaze classification. IET Comput. Vis. 10.

Gaweesh, S.M., Ahmed, M.M., 2019. Evaluating the safety effectiveness of a weather-based variable speed limit for a rural mountainous freeway in Wyoming variable speed limit for a rural mountainous freeway. Journal of Transportation Safety & Security 1–26. https://doi.org/10.1080/19439962.2019.1583707.

Greene, W., 2008. Econometric analysis. Pearson Prentice Hall, Upper Saddle River, New Jersy.

Halton, J., 1960. On the efficiency of evaluating certain quasi-random sequences of points in evaluating multi-dimensional integrals. Numer. Math. 2, 84–90. https://doi.org/10.1007/BF01386213.

Hankey, J.M., Perez, M.A., McClafferty, J.A., 2016. Description of the SHRP 2 naturalistic database and the crash, Near-crash, and baseline data sets. Virginia Tech Transportation Institute.

Hassan, H.M., Shawky, M., Kishta, M., Garib, A.M., Al-Harthei, H.A., 2017. Investigation of drivers' behavior towards speeds using crash data and self-reported questionnaire. Accid. Anal. Prev. 98.

Haydari, A., Zhang, M., Chuah, C.N., 2021. Adversarial Attacks and Defense in Deep Reinforcement Learning (DRL)-Based Traffic Signal Controllers. IEEE Open J. Intelligent Transport. Syst. 2, 402–416. https://doi.org/10.1109/OJITS.2021.3118972.

Hu, W., Donnell, E.T., 2010. Median barrier crash severity: some new insights. Accid. Anal. Prev. 42 (6), 1697–1704. https://doi.org/10.1016/j.aap.2010.04.009.

Khattak, Z.H., Magalotti, M.J., Miller, J.S., Fontaine, M.D., 2017. Using new mode choice model nesting structures to address emerging policy questions: a case study of the Pittsburgh central Business District. Sustainability. https://doi.org/10.3390/su9112120.

Khattak, Z.H., Fontaine, M.D., Boateng, R.A., 2018. Evaluating the impact of adaptive signal control technology on driver stress and behavior using real-world experimental data. Transp. Res. F 58, 133–144. https://doi.org/10.1016/j.trf.2018.06.006.

Khattak, Z., Smith, B.L., Park, H., Fontaine, M.D., 2020a. Cooperative lane control application for fully connected and automated vehicles at multilane freeways. Transp. Res. C 111, 294–317. https://doi.org/10.1016/j.trc.2019.11.007.

Khattak, Z.H., Smith, B.L., Fontaine, M.D., 2020b. Exploratory investigation of disengagements and crashes in autonomous vehicles under mixed traffic: an endogenous switching regime framework. IEEE Trans. Intell. Transp. Syst. https://doi.org/10.1109/TITS.2020.3003527.

Khattak, Z.H., Fonatine, M.D., Li, W., Khattak, A.J., Karnowski, T., 2021. Investigating the relation between instantaneous driving decisions and safety critical events in naturalistic driving environment. Accid. Anal. Prev. 156 https://doi.org/10.1016/j.aap.2021.106086.

Khattak, Z.H., Khattak, A.J., 2021. Spatial and unobserved heterogeneity in consumer preferences for adoption of electric and hybrid vehicles: a Bayesian hierarchical modeling approach. Int. J. Sustain. Transp. https://doi.org/10.1080/15568318.2021.1975327.

Khattak, Z.H., Rios-Torres, J., Fontaine, M., Khattak, A.J., 2022. Inferring safety critical events from vehicle kinematics in naturalistic driving environment: application of deep learning algorithms. J. Intell. Transp. Syst. https://doi.org/10.1080/15472450.2022.2048655.

Khattak, A.J., Wali, B., 2017. Analysis of volatility in driving regimes extracted from basic safety messages transmitted between connected vehicles. Transp. Res. C 84, 48–73. https://doi.org/10.1016/j.trc.2017.08.004.

Kluger, R., Smith, B.L., Park, H., Dailey, D.J., 2016. Identification of safety-critical events using kinematic vehicle data and the discrete fourier transform. Accid. Anal. Prev. 96, 162–168. https://doi.org/10.1016/j.aap.2016.08.006.

Lento, C., Gradojevic, N., Wright, C.S., 2007. Investment information content in bollinger bands? Appl. Financ. Econ. Lett. 3, 4.

Li, N., Busso, C., 2016. Detecting drivers' mirror-checking actions and its application to maneuver and secondary task recognition. IEEE Trans. Intell. Transp. Syst. 17.

Martin, T.L., Solbeck, P.A., Mayers, D.J., Langille, R.M., Buczek, Y., Pelletier, M.R., 2013. A review of alcohol-impaired driving: the role of blood alcohol concentration and complexity of the driving task. J. Forensic Sci 58.

Martin, S., Vora, S., Yuen, K., Trivedi, M.M., 2018. Dynamics of driver's gaze: explorations in behavior modeling and maneuver prediction. IEEE Trans. Intell. Transp. Syst. 3.

Mitchell, R., Bambach, M., Friswell, R., 2014. Work and non-work-related vehicle crashes: the contribution of risky driving practices. Saf. Sci. 68.

Munoz, M., Reimer, B., Lee, J., Mehler, B., Fridman, L., 2016. Distinguishing patterns in drivers visual attention allocation using hidden markov models. Transp. Res. Part F: Traffic Psychology and Behavior 43.

Paolo Busardo, F., Pichini, S., Pellegrini, M., Montana, A., Faro, F.L., 2018. Correlation between blood and oral fluid psychoactive drug concentrations and cognitive impairment in driving under the influence of drugs. Curr. Neuropharmacol. 16.

Perez, M.A., Sudweeks, J.D., Sears, E., Antin, J., Lee, S., Hankey, J.M., Dingus, T.A., 2017. Performance of basic kinematic thresholds in the identification of crash and near-crash events within naturalistic driving data. Accid. Anal. Prev. 103, 10–19. https://doi.org/10.1016/j.aap.2017.03.005.

Rakauskas, M.E., Gugerty, L.J., Ward, N.J., 2004. Effects of naturalistic cell phone conversations on driving performance. J. Saf. Res. 35, 4. https://doi.org/10.1016/j.jsr.2004.06.003.

Regan, M.A., Lee, J.D., Young, K., 2008. Driver distraction: theory, effects, and mitigation. CRC Press.

Rezaei, M., Klette, R., 2014. Look at the Driver, Look at the Road: No Distraction! No Accident!. In: IEEE Conference on Computer Vision and Pattern Recognition. https://doi.org/10.1109/CVPR.2014.24.

Richard, C.M., Lee, J., Atkins, R., Brown, J.L., 2020. Using SHRP2 naturalistic driving data to examine driver speeding behavior. J. Saf. Res.

Ruiz, N., Chong, E., Rehg, J.M., 2018. Fine-grained head pose estimation without keypoints, in: IEEE/CVF Conference on Computer Vision and Pattern Recognition Workshops.

Scott-Parker, B., Oviedo-Trespalacios, O., 2017. Young driver risky behaviour and predictors of crash risk in Australia, New Zealand and Colombia: same but different? Accident Analysis and Prevention 99.

Smorti, M., Guarnieri, S., 2014. Sensation seeking, parental bond, and risky driving in adolescence: some relationships, matter more to girls than boys. Saf. Sci. 70.

Stutts, J., Feaganes., J., Reinfurt., D., Rodgman., E., Hamlett., C., Gish., K., Staplin., L., 2005. Driver's exposure to distractions in their natural environment. Accident Analysis and Prevention 37. doi:https://doi.org/10.1016/j.aap.2005.06.007.

Tavakoli, A., Heydarian, A., 2022. Multimodal driver state modeling through unsupervised learning. Accid. Anal. Prev. 170 https://doi.org/10.1016/j.aap.2022.106640.

Tawari, A., Chen, K.H., Trivedi, M.M., 2014. Where is the driver looking: Analysis of head, eye and iris for robust gaze zone estimation, in: Proc. IEEE Conf. Intell. Transp. Syst.

Tobin, J., 1958. Estimation of relationships for limited dependent Variables. Econometrica 26, 24–26.

Train, K., 2003. Discrete choice methods with simulation, first. ed. Cambridge University Press, Cambridge, United Kingdom.

Ukkusuri, S., Hassan, S., Aziz, H.M.A., 2011. Random Parameter model used to explain effects of built-environment characteristics on pedestrian crash frequency. Transp. Res. Rec. 2237 https://doi.org/10.3141/2237-11.

Vicente, F., Huang, Z., Xiong, X., la Torre, F.D., Zhang, W., Levi, D., 2015. Driver gaze tracking and eyes off the road detection system. IEEE Trans. Intell. Transp. Syst. 16.

Wali, B., Khattak, A.J., 2020. Harnessing ambient sensing & naturalistic driving systems to understand links between driving volatility and crash propensity in school zones – a generalized hierarchical mixed logit framework. Transp. Res. C 114. https://doi.org/10.1016/j.trc.2020.01.028.

Washington, S.P., Karlaftis, M.G., Mannering, F.L., 2011. Statistical and econometric methods for transportation data analysis. CRC Press Taylor And. Francis Group. https://doi.org/10.1198/tech.2004.s238.

Weng, J., Meng, Q., 2012. Effects of environment, vehicle and driver characteristics on risky driving behavior at work zones. Saf. Sci. 50.

Xie, M., Cheng, W., Gill, G.S., Zhou, J., Jia, X., Choi, S., 2018. Investigation of hit-and-run crash occurrence and severity using real-time loop detector data and hierarchical Bayesian binary logit model with random effects. Traffic Inj. Prev. 19, 2. https://doi.org/10.1080/15389588.2017.1371302.
Yan, X., Abdel-Aty, M., Radwan, E., Wang, X., Chilakapati, P., 2008. Validating a driving simulator using surrogate safety measures. Accident Analysis and Prevention 40.
Zhao, Z., Xu, X., Zhang, L., Yan, H., Xu, Y., Zhang, Z., 2020. Driver Distraction detection method based on continuous head pose estimation. Comput. Intell. Neurosci. https://doi.org/10.1155/2020/9606908.